

Pump intensity profiling of vertical-cavity surface-emitting lasers using near-field scanning optical microscopy

G. H. Vander Rhodes,^{a)} J. M. Pomeroy,^{b)} M. S. Ünlü, and B. B. Goldberg

Departments of Physics and Electrical and Computer Engineering, Boston University Photonics Center, Boston, Massachusetts 02215-2421

K. J. Knopp and D. H. Christensen

Optoelectronics Division, National Institute of Standards and Technology, Boulder, Colorado 80303

(Received 14 October 1997; accepted for publication 14 February 1998)

We have mapped the internal pump intensity distribution of an optically pumped vertical-cavity surface-emitting laser. Spontaneous emission from quantum wells placed throughout the distributed Bragg reflectors is correlated to the pump intensity. The emission is monitored along the cleaved edge using the high spatial resolution and shallow depth of field provided by near-field scanning optical microscopy. Our results show a distinct buildup of optical intensity between the mirror stacks. Simulations performed using the transfer matrix method match well with the experimental data. © 1998 American Institute of Physics. [S0003-6951(98)02315-8]

One of the major obstacles to greater efficiency and hence broader use and applications of optically pumped vertical-cavity surface-emitting lasers (VCSELs) is oversensitivity to pump wavelength. Due to the short gain medium, optically pumped VCSELs require distributed Bragg reflectors (DBRs) with not only high reflectance at the lasing wavelength, but also high transmittance at the pump wavelength. Typically, narrow high transmission nodes in the pass band of the DBRs are employed as the window to couple the pump light into the structure.¹ However, temperature sensitivity in the spectral behavior of the DBR structure has required an expensive laser pump with accurate and continuously tunable wavelength control. Recently, new types of DBR mirrors² have been designed which eliminate the need for such a tunable pump source. In the absence of direct measurement, designers have relied on computer simulations in the design and optimization of these novel mirror structures.

In this letter, we describe the use of near-field scanning optical microscopy (NSOM)³ to directly observe the spatial dependence of the optical pump intensity within VCSELs designed and fabricated with a distributed gain medium. The spontaneous emission collected while scanning the near-field aperture along the cleaved edge of the VCSEL provides a direct measurement of the spatial distribution of the pump intensity as a function of wavelength.

The experimental setup is shown in Fig. 1. The pump beam from a Ti:sapphire laser was passed through a beamsplitter to allow the optical power incident on the sample, as well as the return lasing light to be simultaneously monitored. The VCSELs were cleaved and mounted with the cleaved edge facing vertically beneath a tapered single-mode optical fiber.⁴ This near-field aperture was scanned laterally along the cleaved edge while held at a constant height of 10

nm.⁵ Spontaneous emission collected by the probe was sent to the spectrometer.

The VCSELs studied were grown by molecular beam epitaxy (MBE) with a quantum well at every interface of the $\text{Al}_{0.2}\text{Ga}_{0.8}\text{As}/\text{AlAs}$ quarter-wave mirror layers (see Fig. 1, inset).⁶ Generally, VCSELs are grown with active regions only between the two DBR mirrors, whereas the distributed active regions of this design provide a way of sampling the pump field throughout the structure. Additionally, a pump reflector mirror was incorporated to maximize the internal pump field.

The pump light is absorbed in the GaAs quantum wells creating electron-hole pairs. The barriers of the quantum wells inhibit the photogenerated carriers from diffusing out

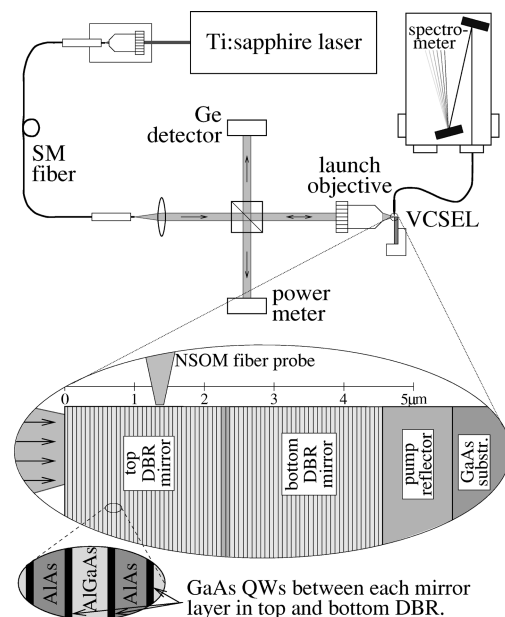


FIG. 1. The top section displays the experimental setup, showing the pump laser, the beamsplitter for optical feedback, the sample at the objective focus, and collection through the NSOM equipment to a spectrometer. The expanded view shows the device structure with the distributed quantum wells and the tip drawn approximately to scale.

^{a)}Electronic mail: gregvr@bu.edu

^{b)}Present address: Department of Physics, Cornell University, Ithaca, NY 14853-2501

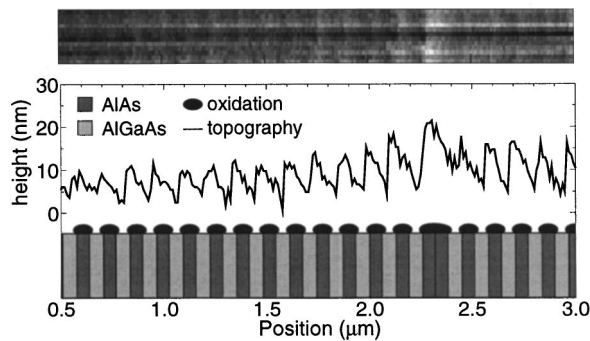


FIG. 2. Topographic shear-force images resolve the height difference due to the increased oxidation of the pure AlAs layers in the mirror stacks. The top image is $200\text{ nm} \times 2.5\text{ }\mu\text{m}$ and the line scan is a representative trace.

of the GaAs active regions, leading to efficient recombination. Diffusion of carriers does take place in the plane of the quantum well, transverse to the pump direction. In the transverse direction perpendicular to both the launch fiber and the NSOM probe (out of the plane of the figure), diffusion is irrelevant because the excitation width is very large compared to the sampling diameter of the probe ($\sim 0.6\text{ }\mu\text{m}$ vs $\sim 0.1\text{ }\mu\text{m}$). Diffusion in the other transverse direction (parallel to the NSOM probe) plays a role in limiting our overall resolution, since emission generated at different depths from the cleaved edge will combine in an unknown manner. Due to the small aperture of the probe, however, the depth of field is limited, reducing this latter effect.

The two main radiative processes are stimulated and spontaneous emission. By monitoring the stimulated emission from the front surface (see Fig. 1), the threshold for lasing was determined. All of the data were taken at pump intensities well below the lasing threshold, where spontaneous emission is the dominant radiative process.

Shear-force feedback⁵ controlled the tip—sample separation and allowed topographic information to be obtained simultaneously with optical data collected through the tip. Figure 2 shows a representative topographic scan, as well as a schematic of the sample. The observed topographic contrast is due to the differing degrees of oxidation of the $\text{Al}_{0.2}\text{Ga}_{0.8}\text{As}$ and AlAs layers of the mirror stack.

Individual spectra were collected at 128 points over a $5\text{ }\mu\text{m}$ scan along the cleaved edge of the device. The data were analyzed by spectrally integrating each spectra and plotting the results as a function of spatial position. Surprisingly, integrating the spectra about the pump wavelength showed very little position dependence. We believe this was due to a large component of scattered pump light being collected by the tip. Such scattering hinders the direct measure of the pump intensity which would have been possible had only evanescent light been collected at the pump wavelength.

However, spontaneous emission is locally generated and therefore not dominated by scattering. Equally important, spontaneous emission is proportional to the pump intensity when the device is operated below lasing threshold. Thus the local total spontaneous emission, obtained by spectrally integrating the entire spontaneous emission spectrum at each point, is used to determine the spatial dependence of the pump intensity.

Figure 3 displays the integrated intensity of the collected

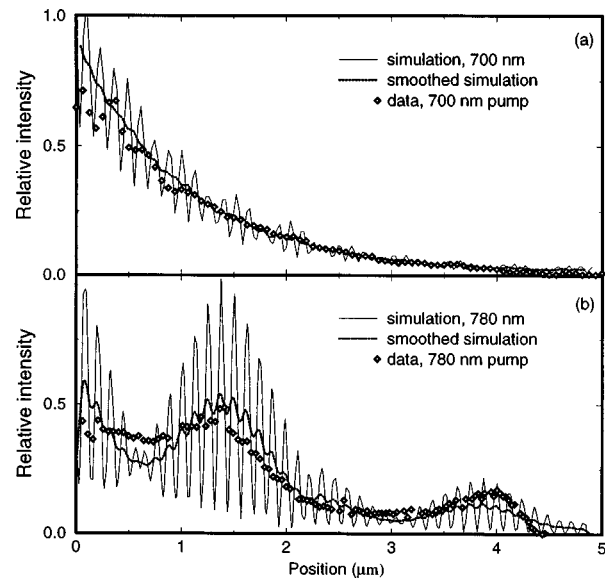


FIG. 3. Integrated spontaneous emission (diamonds), transfer matrix method simulations (solid line), and the simulation convoluted with a Gaussian (dotted line) for 700 and 780 nm pump light wavelengths. The 700 nm data and simulation (a) both show a pump intensity distribution due largely to absorption, since the pump light is energetically above the $\text{Al}_{0.2}\text{Ga}_{0.8}\text{As}$ band gap. For the 780 nm case (b), a buildup of optical intensity inside the layer structure is observed.

spontaneous emission as a function of position along the cleaved edge of the VCSEL for two different wavelengths of pump laser light, one centered within a reflectance minimum (780 nm) and one shifted well away from the lasing wavelength, energetically above the $\text{Al}_{0.2}\text{Ga}_{0.8}\text{As}$ band gap (700 nm).

To help in the interpretation and analysis of the data, detailed simulations were performed for the devices studied. These simulations used the transfer matrix method (TMM),⁷ with layer thicknesses determined from transmission electron microscopy (TEM), x-ray diffraction, and reflectance spectroscopy measurements.⁶ The models used for the complex indices of refraction were taken from Afromowitz⁸ and Terry.⁹

For the above-gap excitation at 700 nm, the spontaneous emission profile is dominated by absorption in the $\text{Al}_{0.2}\text{Ga}_{0.8}\text{As}$, yielding an overall exponential decay into the VCSEL stack, in agreement with the simulation [see Fig. 3(a)]. The correct exponential decay constant validates our measurement technique, since it shows directly the correlation of local spontaneous emission to pump intensity. At excitation wavelengths energetically below the absorption of $\text{Al}_{0.2}\text{Ga}_{0.8}\text{As}$, a distinct buildup of optical intensity within the device is observed. At these longer wavelengths, only the GaAs layers absorb, re-emitting in proportion to their local pump intensity. The Bragg layers are designed to maximize the internal pump field by creating a standing wave, which is both consistent with our data and confirmed by the simulation. Note, however, that the fine structure shown in the simulation (period $\sim 130\text{ nm}$) was not observed. The resolution of NSOM is essentially limited by the diameter of the tip aperture, $\sim 100\text{ nm}$. Also shown in Fig. 3 is the convolution of the simulation with a Gaussian [full width half maximum (FWHM)=100 nm; a simple approximation to the point spread function of the NSOM probe]. The Gaussian convo-

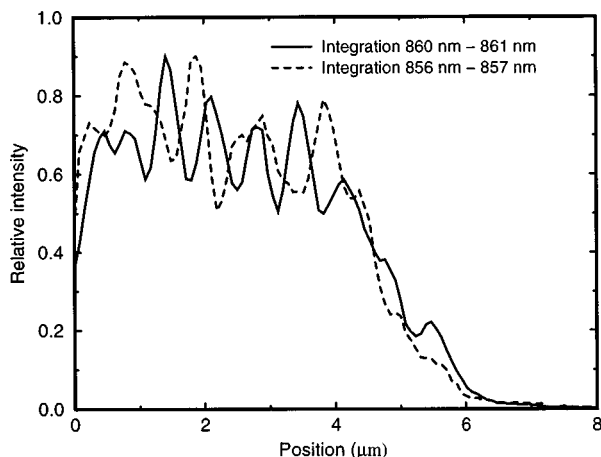


FIG. 4. Two data sets comparing two spectral integration regions for the same pump at a deep launch position below the edge. The solid line is for an integration region from 860 to 861 nm, and the dashed line is for a region from 856 to 857 nm. Both are for a 780 nm pump. The main oscillatory period is about 660 nm which does not correspond to any physical dimensions of the system, including tip-to-sample dimensions. There is a clear position shift between the two data sets. This may be due to a wave guiding effect from light propagating in the plane of the layers.

luted simulation provides solid agreement with the data.

The data discussed above were obtained with the pump light focused just below the edge of the device. When the pump is displaced a significant distance below the surface of the cleaved edge, quite different and interesting spontaneous emission profiles are observed (Fig. 4). In particular, when the pump light was focused 80–100 μm below the sample edge, periodically varying profiles along the scans emerged in the spontaneous emission. The spatial frequencies of the intensity variations do not correspond to a Fabry–Pérot cavity for any of the device's physical dimensions or to a tip-

sample separation. In this region, the spontaneous emission profile became much more sensitive to the spectral integration region. Initial results from a finite difference time domain simulation suggest that the periodicity may be due to waveguiding from light propagating in the plane of the layers. Additional studies of this effect are underway.

In conclusion, the direct mapping of the internal pump intensity distribution of an optically pumped VCSEL structure is made possible by the combination of distributed quantum wells through the DBR mirror stacks and NSOM. This technique is a valuable tool for directly evaluating the spatial distribution of the pump intensity as a function of wavelength. These results will be extended in future work to optimize devices which tailor the thickness of the mirror layers to achieve a desired spectral and spatial function of pump field overlap with the active region.

This work was partially supported by the National Science Foundation under Grant No. ECS-9625236 and by the Department of Education under Grant No. P200A50267-97. The Boston University authors are also very grateful for the continued support of Melles Griot.

¹K. J. Ebeling and T. Hackbarth, *Frequenz* **45**, 207 (1991).

²K. J. Knopp, D. H. Christensen, and J. R. Hill, *IEEE J. Sel. Top. Quantum Electron.* **3**, 366 (1997).

³B. B. Goldberg, M. S. Ünlü, W. D. Herzog, and E. Towe, *IEEE J. Sel. Top. Quantum Electron.* **1**, 1073 (1995).

⁴E. Betzig, J. K. Trautman, T. D. Harris, J. S. Weiner, and R. L. Kostelak, *Science* **251**, 1468 (1991).

⁵K. Karrai and R. D. Grober, *Appl. Phys. Lett.* **66**, 1842 (1995).

⁶D. H. Christensen, C. A. Parsons, J. G. Pellegrino, J. R. Hill, R. S. Rai, S. M. Crochiere, R. K. Hickernell, and D. T. Schaafsma, *Proc. SPIE* **1850**, 115 (1993).

⁷M. Born and E. Wolf, *Principles of Optics* (Macmillan, New York, 1964).

⁸M. A. Fromowitz, *Solid State Commun.* **15**, 59 (1964).

⁹F. L. Terry, Jr., *J. Appl. Phys.* **70**, 409 (1991).